Out-of-plane and in-plane actuation effects on atomic-scale friction

O. Y. Fajardo,[1,][*] E. Gnecco,[2] and J. J. Mazo[1]

[1]*Departamento de Física de la Materia Condensada and Instituto de Ciencia de Materiales de Aragón,*
Consejo Superior de Investigaciones Cientficas, Universidad de Zaragoza, 50009 Zaragoza, Spain
[2]*Instituto Madrileño de Estudios Avanzados, IMDEA Nanociencia, 28049 Madrid, Spain*

The influence of out-of-plane and in-plane contact vibrations and temperature on the friction force acting on a sharp tip elastically pulled on a crystal surface is studied using a generalized Prandtl-Tomlinson model. The average friction force is significantly lowered in a frequency range determined by the "washboard" frequency of the stick-slip motion and the viscous damping accompanying the tip motion. An approximately linear relationship between the actuation amplitude and the effective corrugation of the surface potential is derived in the case of in-plane actuation, extending a similar conclusion for out-of-plane actuation. Temperature causes an additional friction reduction with a scaling relation in formal agreement with the predictions of reaction rate theory in the absence of contact vibrations. In this case the actuation effects can be described by the effective energy or, more accurately, by introducing an effective temperature.

I. INTRODUCTION

Sliding friction is a fundamental problem which is actively being theoretically and experimentally studied at the micro- and nanoscale [1–6]. Recent experimental advances have provided a significant amount of new information on the main characteristics of this phenomenon at small scales. As a consequence, an important theoretical effort to understand qualitatively and quantitatively the experimental outcomes has been activated [7,8]. In this framework, the problem of reducing friction is of utmost importance. Traditional lubricants do not represent a valuable means to achieve this goal in atomic-scale contacts, since the hydrocarbon chains forming the lubricants cause high viscosity when confined in nanometer-sized interstices [9]. An efficient alternative is given by mechanical oscillations applied to the sliding system [10,11]. This has been shown in the atomic force microscopy (AFM) experiments in [12,13], in which a dramatic reduction of friction was observed when the oscillations were applied perpendicularly to the sliding plane (*out of plane*) and frequencies corresponding to mechanical resonances of the probing tip coupled to the surface were chosen. In the same way Lantz *et al*. could drive a silicon tip over a distance of several hundred meters on a polymer surface without observing abrasive wear [14].

Although the influence of out-of-plane oscillations on sliding friction can be related to a periodic decrease of the energy corrugation experienced by the slider [12], systematic theoretical investigations of this effect at different tempera- tures have not been reported so far, which is possibly due to the lack of corresponding experimental results. The same can be said in the case of mechanical vibrations applied along the sliding direction (*in plane*). Recent experiments [15] have shown a significant reduction of the average friction force at the atomic scale caused by lateral vibrations applied to a nanotip elastically pulled on a flat crystal surface. Here, we will try to model this type of *in-plane* actuation. Note that this

_____

*yovany@unizar.es

experimental situation is different from the substrate vibration problem studied numerically in [16–18].

In this work we present detailed numerical simulations of sliding friction on the atomic scale in the presence of out-of- plane and in-plane ac fields. Results are obtained for different values of the four main parameters of the system: frequency and amplitude of the ac field, sliding velocity, and temperature. Friction force is reduced in well-defined frequency windows, and the effect is enhanced at increasing temperature and actuation amplitude. An analytical formula explaining the gradual transition from stick-slip to superlubricity at $T = 0$ K is also derived. Regarding the thermal behavior of the system, we show how our numeric results scale following the law given by reaction rate theory, commonly used to predict the temperature dependence of atomic-scale friction in the absence of mechanical vibrations. Quantitative agreement is also obtained if appropriate effective parameters are introduced.

II. THE PRANDTL-TOMLINSON MODEL WITH AC ACTUATION

In order to analyze ac-actuation effects on atomic-scale friction, we start from the one-dimensional Prandtl-Tomlinson (PT) model including thermal effects [19–26]:

$$m\frac{d^2x}{dt^2} + m\gamma\frac{dx}{dt} + \frac{\partial U(R,x)}{\partial x} = \xi(t),$$
$$U(R,x) = V_{el}(R,x) + V_{int}(x).$$
(1)

Here, a single particle of mass m, representing the AFM tip apex, is driven along a periodic substrate, experiencing an effective potential $U(R,x)$. This potential includes an elastic contribution, V_{el}, and a tip-substrate interaction term, V_{int}. The first term describes the combined effect of the lateral deformation of the elastic cantilever support (moving at a constant velocity v_s, so its position is $R(t) = R_0 + v_s t$, the deformation of the tip apex, and the sample surface: $V_{el} = k(v_s t - x)^2/2$, where k is an effective spring constant [27,28]. In the first-order approximation the tip-surface interaction is $V_{int}(x) = -U_0 \cos(2\pi x/a)$, where a is the spatial periodicity
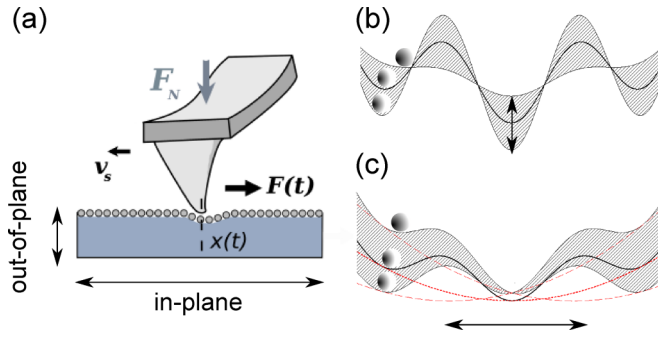
FIG. 1. (Color online) (a) Sketch of a friction force microscopy experiment with actuation. A sharp tip is set into contact with a crystal surface under a given load F_N and laterally pulled by a flexible cantilever at a constant velocity v_s. The surface sample (or, equivalently, the free end of the cantilever) is shaken either in the normal or in the lateral direction. Portraits of the potential energy $U(R,x)$ when the cantilever is set in motion are shown for (b) out-of-plane actuation and (c) in-plane actuation (in this case the red lines show the time variation of the elastic energy V_{el}). The tip apex (represented by a gray ball) lies in a local minimum of the total potential $U(R,x)$.

of the surface lattice. The random noise term $\xi(t)$ is related to the temperature T by the fluctuation-dissipation relation $\langle \xi(t)\xi(t')\rangle = 2m\gamma k_B T \delta(t-t')$, where γ is a microscopic friction coefficient describing the coupling with phonon and possible electron oscillations in the substrate, and k_B is the Boltzmann constant.

Ac-actuation effects are taken into account in two different ways (Fig. 1). Out-of-plane actuation acts perpendicularly to the sliding plane. As discussed in [12,29], this effect can be modeled assuming that the interaction potential oscillates as a function of time around the value U_0 (fixed by the normal load F_N) with the actuation frequency f and a relative amplitude α [Fig. 1(b)]:

$$V_{int}(x,t) = -U_0(1 + \alpha \cos 2\pi f t) \cos\left(\frac{2\pi x}{a}\right). \quad (2)$$

In the present work we model *in-plane* actuation by adding a shaking term to the support position $R(t)$, so that the elastic energy reads [30,31]

$$V_{el}(x,t) = \frac{k}{2}(v_s t + \beta a \, \sin 2\pi f t - x)^2. \quad (3)$$

In Eq. (3) the parameter β quantifies the relative amplitude of the oscillations. The variation of the total potential $U(R,x,t)$ during an oscillation is sketched in Fig. 1(c).

In the following, we are interested in estimating the mean value $\langle F \rangle$ of the instantaneous lateral force $F(t) = k[R(t) - x(t)]$, as measured by the AFM, at different model parameters, e.g., the amplitude and frequency of the ac-actuation term, scan velocity, and temperature. In the framework of the PT model, the quantity $\langle F \rangle$ can be identified with the kinetic friction force acting on the tip. To this end we have integrated the equations of motion of the system, Eq. (1), and averaged the results over many periods of the ac field. Nondimensional equations are introduced by measuring energy in units of U_0, length in units of the lattice spacing ($\tilde{x} = 2\pi x/a$), and time in units of
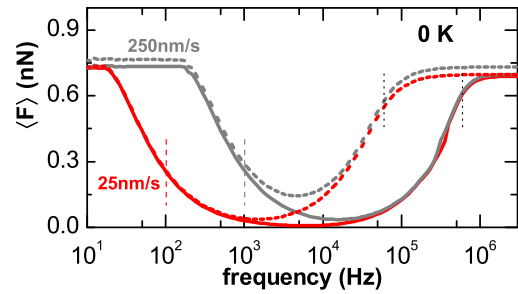

FIG. 2. (Color online) Damping and velocity effects on the friction force in the presence of out-of-plane actuation. We show the mean friction force as a function of the actuation frequency f and for two velocity values, $v_s = 25$ (red line) and 250 nm/s (gray line). Continuous and dashed lines correspond to the nondimensional damping values $\tilde{\gamma} = 1$ and 10, respectively. The vertical dashed lines indicate the frequencies $f_{wb} = v_s/a$ and $\omega_p/2\pi\tilde{\gamma}$ associated with both velocities and dampings. These lines define the limits for which the reduction of the friction becomes effective.

the resonance frequency of the point mass in the wells of the sinusoidal potential ($\tau = \omega_p t$ with $\omega_p = 2\pi\sqrt{U_0/ma^2}$). Then $\tilde{\gamma} = \gamma/\omega_p$, $\tilde{k} = 1/\eta = ka^2/(4\pi^2 U_0)$ and $\tilde{v}_s = v_s\sqrt{m/U_0}$ are the scaled damping, spring constant, and velocity, respectively.

For the parameter values we have chosen $m = 2.0 \times 10^{-12}$ kg, $a = 0.246$ nm, and $k = 3.73$ N/m. For v_s we have used 25 nm/s, except for the results shown in Fig. 2, in which two values, $v_s = 25$ and 250 nm/s, have been chosen. With respect to the potential amplitude, $U_0 = 0.25$ eV. This set of values corresponds to typical parameters used in experiments and theoretical works on the topic [21,24,32]. For our choice of parameter values, $\omega_p/2\pi = 0.6$ MHz and $\eta = 7.0$.

III. ACTUATION EFFECTS AT ZERO TEMPERATURE

We first review results for ac actuation without thermal effects. Figure 2 presents the most important ones, where we have chosen to show the effect of out-of-plane actuation at $\alpha = 0.9$, a large amplitude value. Results for smaller α and in-plane actuation are qualitatively similar and are summarized in Sec. IV. The most important finding is the existence of a wide medium-frequency range ($f \sim$ a few kHz) where the friction force is importantly reduced and almost suppressed for intense enough actuation. We notice that the lower bound of this reduced friction zone is determined by the support velocity v_s, and the upper bound is determined by the effective damping γ. Indeed, friction reduction is observed for actuation frequencies f such that

$$v_s/a \leqslant f \leqslant \omega_p/(2\pi\tilde{\gamma}). \quad (4)$$

The support velocity v_s defines a characteristic frequency of the system, the washboard frequency $f_{wb} = v_s/a$ associated to the time needed to advance one period of the substrate potential. Thus, for frequency values $f \ll f_{wb}$, actuation is not effective. This is not the case when f approaches f_{wb}, as seen in Fig. 2 (in which f_{wb} is marked by vertical dashed lines for each velocity value). In addition, damping and inertial effects do not play an important role in this low-frequency range.

At high frequency we can consider the system as an overdamped forced oscillator. The tip is unable to follow the external field for $2\pi\gamma f/\omega_p^2 \gg 1$, which corresponds to $f \gg 0.6/\widetilde{\gamma}$ MHz with our choice of values. In this high-frequency regime the support velocity v_s does not play an important role.

A. Dependence of friction on the actuation amplitude

One of the most important questions is to determine how the overall friction depends on the actuation field amplitude. This issue is studied in Fig. 3. Here the mean friction force $\langle F \rangle$ is represented as a function of the amplitude oscillation for two frequency values with and without thermal effects. Figure 3 shows the decrease of the force $\langle F \rangle$ as a function of α or β down to a "frictionless" superlubricity regime. As shown in Fig. 3, the magnitude of the reduction effect varies almost linearly with the amplitude of the actuation field. We note that this effect can be reproduced by defining an effective amplitude barrier U_0^{eff}, and thus an effective PT parameter η_{eff}, corresponding to the η value which gives the same friction force of the original system with an applied actuation field of intensity α (or β). In other words, $\langle F \rangle(\eta, \alpha) = \langle F \rangle(\eta^{\text{eff}}, \alpha = 0)$ (and similarly for β). This η^{eff} can be computed for each value of α or β and f.

At $T = 0$ analytical expressions for the dependence of η_{eff} with the actuation amplitude can be derived. These expressions are effective at the frequency values corresponding to the minima of the friction force versus frequency curves. In the case of out-of-plane actuation, Socoliuc *et al.* [12] observed that

$$\eta_{\text{eff}}(\alpha) \simeq \eta(1 - \alpha), \tag{5}$$

considering the minimum value of the energy barrier for slippage which is reached during an oscillation. Similarly, in

FIG. 4. Theoretical and numerical comparison of the effective PT parameter for different values of the actuation amplitude at $f = 5$ kHz and $T = 0$.

the case of in-plane-actuation, we have found that

$$\eta_{\text{eff}}(\beta) \simeq \eta - 2\pi\beta. \tag{6}$$

Equation (6) is obtained from the theoretical analysis presented in the Appendix. There, assuming that the slip event occurs at the maximum elongation of the tip-support spring, we are able to predict the dependence of the friction force with the actuation field amplitude for the case of *in-plane* actuation and zero temperature, Eq. (A6). This expression is derived considering the first nonzero terms in the series expansion in β of the "takeoff" and "landing" positions of the tip slipping across the surface lattice and the corresponding variation of the total energy U. The predicted result is plotted in Fig. 3(b), which corresponds to a frequency for which friction is strongly reduced in the system. Furthermore, Fig. 4 shows that, if one wants to keep to a linear dependence on η, a good approximation is obtained using $\eta_{\text{eff}} = 7.0 - 6.44\alpha$ and $7.0 - 6.0\beta$. The numeric coefficients appearing in these expressions are only slightly different from those in Eqs. (5) and (6).

IV. THERMAL EFFECTS

It is well known that friction at the atomic scale can be reduced by thermal vibrations [21]. At finite temperature the tip slippage is anticipated, which decreases the average friction force. This is also the case in which an actuation force is applied. Figures 3–7 show the dependence of the mean friction force on the actuation frequency f, the actuation field amplitude α or β, and the temperature T. These figures reveal the existence of a frequency range at which the actuation effectively reduces friction, an almost linear dependence of the friction force on the actuation amplitude, and they also describe the influence of thermal vibrations on the friction force.

In particular, Fig. 3 compares the dependence of the friction with the actuation amplitude at $T = 0$ and 300 K. It can be seen that an almost linear decrease holds also in the presence of thermal effects.

The change in the friction versus actuation frequency curves when thermal effects are introduced is shown in Fig. 5. As expected, an important reduction in the friction
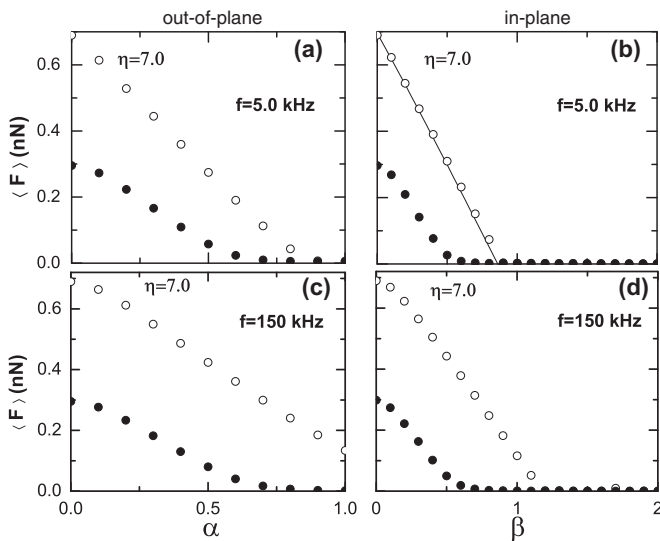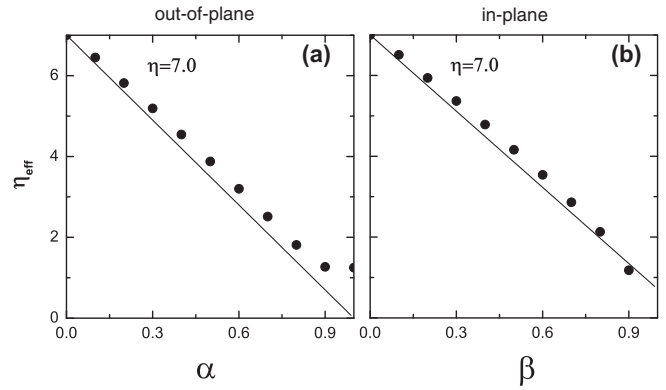

FIG. 3. Friction force $\langle F \rangle$ for different values of the actuation amplitude for the frequencies values $f = 5$ and 150 kHz. (a) and (c) The out-of-plane actuation case. (b) and (d) The in-plane actuation case. In all cases $T = 0$ K for open circles and 300 K for solid circles. The full line in figure (b) stands for the theoretical prediction of Eq. (A6) up to the third term on the right-hand side.
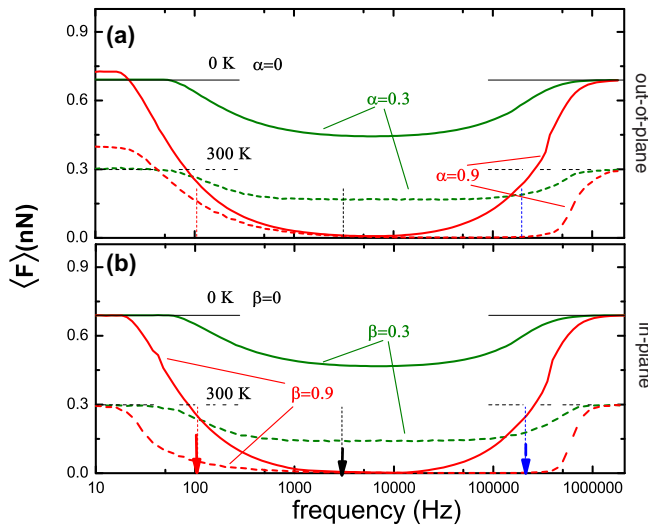
FIG. 5. (Color online) Friction force as a function of the actuation frequency for $T = 0$ (continuous lines) and 300 K (dashed lines). $v_s = 25$ nm/s and $\widetilde{\gamma} = 1$. (a) Out-of-plane actuation curves for $\alpha = 0.3$ (upper green lines) and 0.9 (lower red lines). (b) Results for in-plane actuation for $\beta = 0.3$ (upper green lines) and 0.9 (lower red lines). Thin vertical lines correspond to $v_s/a = 101$ Hz and two specific frequency values used in our study, $f = 5$ and 150 kHz.

force is observed. This reduction adds to that caused by the ac-actuation on the tip. We also observe that the frequency boundaries of the region of effective friction reduction are not modified at finite temperature.

A. Scaling behavior

To account for the temperature dependence of the mean friction force in the absence of ac actuation, the following law has been proposed [19,21]:

$$\langle F \rangle = F_c - B\, T^{2/3}\, [\ln(C\, T/v_s)]^{2/3}, \tag{7}$$

where F_c, B, and C are constants defined by the system parameters. Equation (7) can be obtained from the Kramers expression for the escape rate of a particle out of a metastable well, evaluated in the overdamped limit.

The case of ac actuation force is much more complex. In fact, no simple expression for the escape rate has been derived in the presence of ac fields [33–35]. As a consequence, a simple relation for the friction force reduction is also missing. Nevertheless, as substantiated by the numerical simulation results detailed below, we observe that the formula Eq. (7), with different values of the parameters F_c, B, and C, is still valid when both ac actuation and thermal effects are included. This can be seen in Fig. 6, in which results for both out-of-plane and in-plane actuation and two different frequency values are shown. Here, the same scaling relation predicted in the absence of actuation fields,

$$\frac{(F_c - F)^{3/2}}{T} \propto \log \frac{v_s}{T} + \text{const}, $$

is found to hold. In Fig. 6 both actuation amplitudes α and β were set equal to 0.3, a moderate value. This scaling only
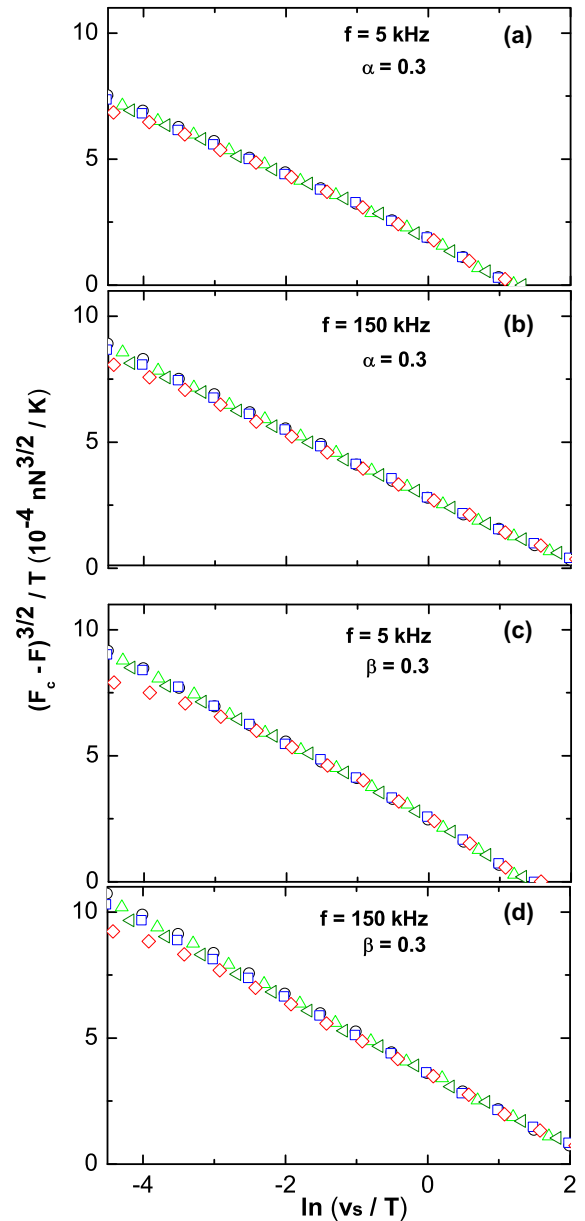

FIG. 6. (Color online) Scaling behavior of the friction force in the presence of out-of-plane actuation with $\alpha = 0.3$ and (a) $f = 5$ kHz and (b) $f = 150$ kHz and in the presence of in-plane actuation with $\beta = 0.3$ and (c) $f = 5$ kHz and (d) $f = 150$ kHz. Circles, triangles, squares, lateral triangles, and diamonds correspond to the temperatures $T = 150, 200, 250, 293$, and 373 K, respectively.

breaks down for large enough actuation fields, when F goes to zero and the superlubricity regime is reached (see Fig. 3).

B. Effective temperature

Our major finding is that the ac-actuation effect can be described by introducing new effective parameters of the system. This approach is found to be valid in a wide range of actuation parameter values and in the stick-slip regime of the system. In Sec. III A we introduced an effective PT parameter, η_{eff}, which at zero temperature accounts for the friction reduction in the system when ac fields are applied.
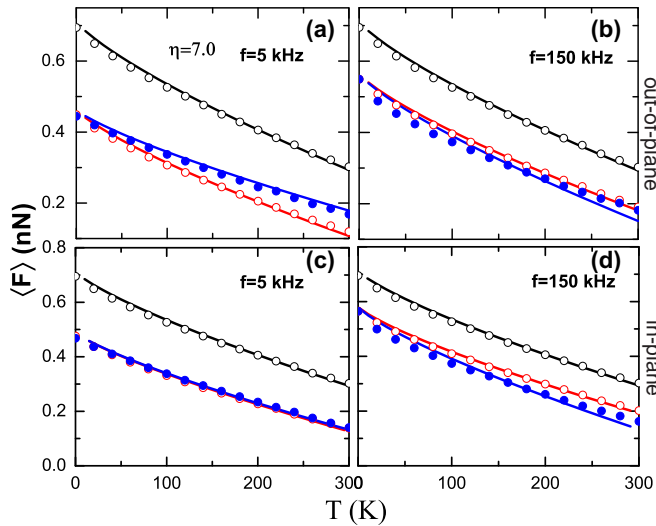
FIG. 7. (Color online) Friction force at different temperatures with and without ac actuation (either out of plane or in plane): simulations without actuation (open black circles) for $\eta = 7.0$ and fits from Sang's theory (black curves); simulations without actuation using an effective energy corrugation (open red circles) and fits from Sang's theory (red curves); and simulation with actuation (solid blue circles) and fits using an effective energy corrugation and effective temperature T_{eff} (blue curves) with $\theta = 0.82, 1.1, 0.98$, and 1.2 from (a) to (d), respectively.

Now, guided by the scaling relations we have found, and by the existing theories, we will extend our discussion to the understanding of the friction versus temperature curves.

Figure 7 summarizes our conclusion. Open black circles describe the temperature dependence of the friction force in the absence of ac actuation. We see that the friction force is well fitted by Eq. (7) of the Sang *et al.* theory [21] (black lines in Fig. 7). The solid blue circles in Fig. 7 show the

temperature dependence of the friction force in the presence of actuation. These points are approximately fitted by the red curves, corresponding to Eq. (7) with η replaced by the parameter η_{eff} discussed in the previous section.

However, as expected from the obtained scaling dependence, a much better agreement is obtained if, in addition, an effective temperature $T_{\text{eff}} = \theta T$ is introduced (where θ is close to 1). This is shown by the blue curves, corresponding to the equation

$$\langle F \rangle = F_c - B\, T_{\text{eff}}^{2/3}\, [\ln(C\, T_{\text{eff}}/v_s)]^{2/3}, \qquad (8)$$

where the parameters F_c, B, and C are calculated in the same way as in Eq. (7), using the obtained effective value for the energy of the corrugation potential. Only at high values of the actuation amplitude, strong nonlinear effects destroy the scaling relationship between the real temperature T of the system and the effective temperature T_{eff}.

C. Force-velocity curves

To conclude, we present in Fig. 8 additional results on the friction force versus velocity dependence with ac actuation and thermal effects. We have to remark that in this case we plot the reduced friction force $\langle F^* \rangle = \langle F \rangle - \gamma m v_s$ in order to suppress the viscous drag contribution which dominates at high velocities. Damping has been fixed to $\widetilde{\gamma} = 1$. The inset of Fig. 8(a) shows a typical force-frequency curve, similar to those shown in Fig. 2(a). Figure 8(a) shows a log-log surface plot at $T = 0$ of the reduced friction force as a function of dragging velocity v_s and actuation frequency f. As previously discussed, the low friction region narrows as the support velocity increases. This is due to the increasing value of f_{wb}, which gives the onset of the small friction zone, whereas the high-frequency boundary, which basically depends on the $\omega_p/\widetilde{\gamma}$ ratio, remains constant.

Figure 8(b) shows the friction versus velocity curves at different frequency values and temperatures $T = 0$ and 300 K.
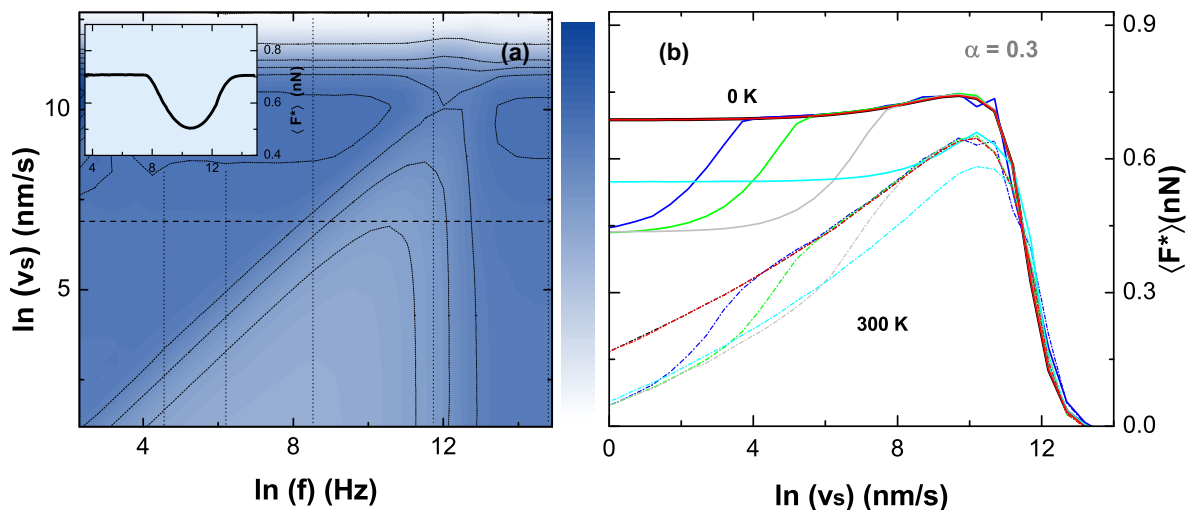

FIG. 8. (Color online) (a) Isosurface of the friction force as a function of the logarithm of the tip velocity and the excitation frequency in the case of out-of-plane actuation without thermal effects. Inset: A profile of the friction force along the dashed line marked on the isosurface. (b) The friction force as a function of the tip velocity for different frequency values: $f = 0$ (black), 100 (blue), 500 (green), 5×10^3 (light gray), 150×10^3 (cyan), and 3×10^6 (red) Hz. Continuous curves correspond to $T = 0$ K, and dashed curves correspond to $T = 300$ K. In all cases $\alpha = 0.3$ and $\widetilde{\gamma} = 1$.

Such curves can be easily understood with the help of Fig. 8(a), in which we have marked the chosen frequency values. There, thermal effects on the velocity dependence of the friction force are explicitly plotted. Such effects can be understood with the help of Eq. (8) after the introduction of the effective parameters.

V. CONCLUSIONS

We have made a detailed numerical analysis of in-plane and out-of-plane ac actuation effects on the average friction force of a system at the atomic scale, in the framework of a one-dimensional Prandtl-Tomlinson model including thermal effects. Our work shows that in-plane and out-of-plane actuation give pretty similar results. This can be qualitatively understood from Figs. 1(b) and 1(c). In both cases one observes a periodic reduction of the energy barrier to be overcome by the tip. While this is not surprising in the case of out-of-plane actuation, the same effect for in-plane actuation is less obvious and quite remarkable.

Actuation forces are effective for friction reduction in an intermediate range of frequencies. This range is limited by the washboard frequency of the system, associated to the motion at a given velocity over a periodic potential, and by the frequency value at which the relaxation time of the system becomes comparable to the actuation period so that the system becomes unable to follow the dynamics of the ac force. The first frequency is essentially given by the drag velocity of the support, v_s; the second one is determined by the effective damping γ of the system.

Having seen that the ac actuation effect can be understood in terms of a reduction of the effective barrier of the system which accounts for a reduction of the PT parameter, η, thermal effects cause an additional friction reduction which is well reproduced by the Sang expression of Eq. (7). A better agreement is obtained introducing an effective temperature weakly different from the real one.

The friction reduction caused by in-plane oscillations and the scaling relations predicted by our work remain to be fully tested experimentally. It is interesting to observe that, in the absence of ac actuation, Jansen *et al.* found a good agreement with the thermally activated PT model at any temperature between 100 and 300 K on graphite [25]. However, they also observed a decrease of friction with decreasing T below 130 K on NaCl [36], which was related to the formation of multiasperity contacts. Superimposing lateral vibrations at different frequencies while sliding may help to shed light on this intriguing effect.

Other actuation schemes have been recently theoretically studied. Interesting results using simulations of many-atoms confined between two plates, one sliding and the other vertically vibrating, also showed friction suppression at suitable vibration frequency and amplitude [37].

APPENDIX: ANALYTICAL EXPRESSIONS FOR ATOMIC STICK-SLIP WITH IN-PLANE ACTUATION

Here we will present an analytical approach to $\langle F \rangle(\eta,\beta)$ and discuss how Eq. (6) can be derived as a first approximation for the not trivial dependence of the average friction force on the parameter values $\eta = 4\pi^2 U_0/(ka^2)$ and β. If the driving velocity is sufficiently low, the tip position x at a given time t is given by the equilibrium condition $\partial U/\partial x = 0$. In the absence of vibrations,

$$U(x,t) = -\eta \cos x + \frac{(v_s t - x)^2}{2} \tag{A1}$$

(in nondimensional units), and the previous condition becomes

$$\eta \sin x + x - vt = 0. \tag{A2}$$

When the spring is pulled along the scan direction the tip slightly moves forward. When the tip reaches the critical position x_c defined by $\partial^2 U/\partial x^2 = 0$, the equilibrium becomes unstable and the tip jumps. The critical position is given by

$$\eta \cos x_c + 1 = 0. \tag{A3}$$

Combining Eqs. (A2) and (A3) we get for the critical time t_c

$$vt_c = \sqrt{\eta^2 - 1} + \arccos(-1/\eta) \equiv f(\eta).$$

When in-plane vibrations are switched on, the jump will be anticipated. In order to calculate the critical time in this case, we have to replace vt with $vt + \beta$ in Eq. (A2). This substitution makes sense provided that the spring elongation does not change significantly during the period $1/f$ of the oscillations, which is the case if the condition Eq. (4) is satisfied.

After jumping, the tip ends in the next minimum x_c' of the total potential U. If $\eta \gg 1$ the coordinates x_c and x_c' of the takeoff and landing points are approximately equal to $\pi/2$ and $5\pi/2$, respectively.

As a next step, assuming that η is large enough, we expand the function $f(\eta)$ introducing the variable $\nu = 1/\sqrt{\eta}$:

$$f(\eta) = \frac{1}{\nu^2} + \frac{\pi}{2} + \cdots.$$

The takeoff and landing positions are then given by

$$x_c = \frac{\pi}{2} - 2\sqrt{\pi\beta}\,\nu + \nu^2 - \frac{\pi^{3/2}\beta^{3/2}}{3}\nu^3 + \frac{2\pi\beta}{3}\nu^4 - \cdots \tag{A4}$$

and

$$x_c' = \frac{5\pi}{2} - 2\sqrt{\pi(1+\beta)}\,\nu + \nu^2 - \frac{\pi^{3/2}}{3}(1+\beta)^{3/2}\nu^3 + \frac{2\pi}{3}(1+\beta)\nu^4 - \cdots, \tag{A5}$$

respectively.

At each jump the energy amount $\Delta U = U(x_c) - U(x_c')$ is released from the contact region in the form of phononic or electronic excitations. The mean friction force, which we identify as the lateral force averaged over several lattice

constants, can be simply determined from this quantity as $\langle F \rangle = \Delta U / 2\pi$, in nondimensional units. Substituting the expressions Eqs. (A4) and (A5) in Eq. (A1) we finally get

$$\langle F \rangle(\eta, \beta) = \eta - \pi(1 + 2\beta) + \frac{4}{3}\sqrt{\frac{\pi}{\eta}}[(1 + \beta)^{3/2} - \beta^{3/2}]$$
$$- \frac{1}{2\eta} + \frac{2}{15}\left(\frac{\pi}{\eta}\right)^{3/2}[(1 + \beta)^{5/2} - \beta^{5/2}] - \cdots . \tag{A6}$$

Note that Eqs. (A4)–(A6) generalize Eqs. (15)–(17) in [38] when $\beta \neq 0$. Previous equations are dimensionless. In standard units, the right-hand sides of the equations defining the critical positions and the friction force are multiplied by the factors $(a/2\pi)$ and $(ka/2\pi)$, respectively.

In particular, when $\beta = 0$,

$$\langle F \rangle(\eta, 0) = \eta - \pi + \frac{4}{3}\sqrt{\frac{\pi}{\eta}} - \frac{1}{2\eta} + \frac{2}{15}\left(\frac{\pi}{\eta}\right)^{3/2} - \cdots .$$

At the first order in β, we can thus say that

$$\langle F \rangle(\eta, \beta) \simeq \langle F \rangle(\eta - 2\pi\beta, 0),$$

i.e., the effect of lateral vibrations on the support can be approximately taken into account replacing the parameter η with $\eta_{\text{eff}} = \eta - 2\pi\beta$.

[1] B. Bhushan, *Introduction to Tribology* (Wiley, New York, 2013).
[2] M. Urbakh and E. Meyer, Nature Materials **9**, 8 (2010).
[3] E. Gnecco and E. Meyer, *Fundamentals of Friction and Wear on the Nanoscale* (Springer, New York, 2007).
[4] M. Urbakh, J. Klafter, D. Gourdon, and J. Israelachvili, Nature (London) **430**, 525 (2004).
[5] B. N. J. Persson and E. Tosatti, *Physics of Sliding Friction* (Kluwer Academic, Norwell, 1992).
[6] I. L. Singer and H. M. Pollock, *Fundamentals of Frictions: Macroscopic and Microscopic Processes* (Kluwer Academic, Norwell, 1992).
[7] Y. Dong, A. Vadakkepatt, and A. Martini, Tribol. Lett. **44**, 367 (2011).
[8] A. Vanossi, N. Manini, M. Urbakh, S. Zapperi, and E. Tosatti, Rev. Mod. Phys. **85**, 529 (2013).
[9] Y. Z. Hu and S. Granick, Trib. Lett. **5**, 81 (1998).
[10] F. Dinelli, S. K. Biswas, G. A. D. Briggs, and O. V. Kolosov, Appl. Phys. Lett. **71**, 1177 (1997).
[11] E. Riedo, E. Gnecco, R. Bennewitz, E. Meyer, and H. Brune, Phys. Rev. Lett. **91**, 084502 (2003).
[12] A. Socoliuc, E. Gnecco, S. Maier, O. Pfeiffer, A. Baratoff, R. Bennewitz, and E. Meyer, Science **313**, 207 (2006).
[13] S. Jeon, T. Thundant, and Y. Braiman, Appl. Phys. Lett. **88**, 214102 (2006).
[14] M. A. Lantz, D. Wiesmann, and B. Gotsmann, Nature Nanotech. **4**, 586 (2009).
[15] R. Roth, O. Y. Fajardo, J. J. Mazo, E. Meyer, and E. Gnecco, arXiv:1402.3605 [Appl. Phys. Lett. (to be published)].
[16] Z. Tshiprut, A. E. Filippov, and M. Urbakh, Phys. Rev. Lett. **95**, 016101 (2005); Tribology Int. **40**, 967 (2007).
[17] R. Guerra, A. Vanossi, and M. Urbakh, Phys. Rev. E **78**, 036110 (2008).
[18] Y. Liu, L. Shen, and Q. Zheng, Int. J. Multiscale Comput. Eng. **11**, 27 (2013).
[19] L. Prandtl, Z. Angew. Math. Phys. **8**, 85 (1928).

[20] E. Gnecco, R. Bennewitz, T. Gyalog, C. Loppacher, M. Bammerlin, E. Meyer, and H. J. Güntherodt, Phys. Rev. Lett. **84**, 1172 (2000).
[21] Y. Sang, M. Dube, and M. Grant, Phys. Rev. Lett. **87**, 174301 (2001).
[22] S. Sills and R. M. Overney, Phys. Rev. Lett. **91**, 095501 (2003).
[23] M. Reguzzoni, M. Ferrario, S. Zapperi, and M. C. Righi, Proc. Nat. Acad. Sci. USA **107**, 1311 (2009).
[24] O. Y. Fajardo and J. J. Mazo, Phys. Rev. B **82**, 035435 (2010).
[25] L. Jansen, H. Hölscher, H. Fuchs, and A. Schirmeisen, Phys. Rev. Lett. **104**, 256101 (2010).
[26] M. H. Müser, Phys. Rev. B **84**, 125419 (2011).
[27] R. W. Carpick, D. F. Ogletree, and M. Salmeron, Appl. Phys. Lett. **70**, 1548 (1997).
[28] M. A. Lantz, S. J. O'Shea, M. E. Welland, and K. L. Johnson, Phys. Rev. B **55**, 10776 (1997).
[29] H. Iizuka, J. Nakamura, and A. Natori, Phys. Rev. B **80**, 155449 (2009).
[30] M. Igarashi, J. Nakamura, and A. Natori, Jpn. J. Appl. Phys. **46**, 5591 (2007).
[31] R. Capozza, S. M. Rubinstein, I. Barel, M. Urbakh, and J. Fineberg, Phys. Rev. Lett. **107**, 024301 (2011).
[32] O. Y. Fajardo and J. J. Mazo, J. Phys.: Condens. Matt. **23**, 355008 (2011).
[33] J. Lehmann, P. Reimann, and P. Hänggi, Phys. Rev. Lett. **84**, 1639 (2000); Phys. Rev. E **62**, 6282 (2000).
[34] R. S. Maier and D. L. Stein, Phys. Rev. Lett. **86**, 3942 (2001).
[35] S. Getfert and P. Reimann, Chem. Phys. **375**, 386 (2010).
[36] I. Barel, M. Urbakh, L. Jansen, and A. Schirmeisen, Phys. Rev. B **84**, 115417 (2011).
[37] R. Capozza, A. Vanossi, A. Vezzani, and S. Zapperi, Phys. Rev. Lett. **103**, 085502 (2009).
[38] E. Gnecco, R. Roth, and A. Baratoff, Phys. Rev. B **86**, 035443 (2012).